PPS
Paper
www.rsc.org/pps

Solvent and temperature effects on the deactivation pathways of excited ion pairs produced *via* photoinduced proton transfer †

László Biczók,*[a] Pierre Valat[b] and Véronique Wintgens[b]

[a] *Chemical Research Center, Hungarian Academy of Sciences, P.O. Box 17, 1525 Budapest, Hungary. E-mail: biczok@chemres.hu*
[b] *Laboratoire des Recherche sur les Polymeres, C.N.R.S., UMR C7581, 2, 8 rue H. Dunant, 94320 Thiais, France*

Received 30th September 2002, Accepted 28th October 2002
First published as an Advance Article on the web 8th January 2003

The kinetics of the energy dissipation pathways of the excited ion pairs formed upon light absorption of the hydrogen bonded complex between *N*-methyl-3-hydroxynaphthalimide (3HONI) and 1-methyl-imidazole (MIm) has been studied in a wide temperature range in solvents of various polarities. In polar media such as butyronitrile, three emitting species are found which are assigned as hydrogen bonded, solvent separated and free ion pairs. In contrast, less polar solvents do not favour free ion pair formation, and reversible transition occurs between the excited hydrogen bonded (HBIP) and solvent separated (SSIP) ion pairs around room temperature. Systematic steady-state and time-resolved fluorescence measurements combined with computer modelling enabled the deduction of the kinetic parameters for all excited state deactivation processes in solvents of moderate polarity. The Arrhenius parameters of the interconversion between the ion pairs, the A-factor for the radiationless deactivation of SSIP and the radiative rate constant of HBIP diminish with the increasing dielectric constant of the media. The enthalpy and the entropy change in the SSIP formation from HBIP become less negative in more polar solvents. Going from ethyl acetate to CH_2Cl_2 the most profound decrease (more than three orders of magnitude) is observed for the A-factor of SSIP ⟶ HBIP reaction.

Introduction

Ion pairing of organic salts has received a considerable interest[1] since Winstein[2] and Sadek[3] introduced the concept of "loose" and "tight" ion pairs. Y. Marcus distinguished three types of ion pairs, which differ in the interionic distance and the structure of solvate shell.[4] Effects of counter ion, solvent and temperature have been examined with various techniques like conductivity, EPR, NMR, IR, Raman and absorption spectroscopy. Most of the knowledge on ion pairs stems from ground state studies; much less attention has been devoted to the ion pair recombination and separation processes in the excited state. The large overlap among the absorption of the various types of ground state ion pairs renders more difficult the study of their excited state reactions. Moreover, the shift in the ground state equilibria caused by solvent and temperature effects complicates the interpretation of the fluorescence characteristics. In spite of the lack of resolved spectral bands, it was possible to prove the coexistence of different excited ion pairs with a time-resolved fluorescence technique.[5,6] Dual emission was observed from ion pairs in the 1-naphthol–aliphatic amine system in non-polar rigid matrices at 77 K, which was ascribed to contact and separated ion pairs.[7,8] The formation and decay pathways of these species could be examined only at low temperature because both static and dynamic quenching was found to be very efficient[9] above *ca.* 160 K.

There is a controversy in the literature on whether contact ion pairs convert to solvent separated or free ion pairs on excitation. Vos *et al.* proposed that ground state contact ion pairs are transformed immediately into solvent separated ion pairs in the excited state.[10] Hogen-Esch *et al.* suggested that light absorption could lead to dissociation into free ions.[11] It was also concluded[6] that the exchange between excited contact and solvent separated ion pairs was slow compared to the fluorescence time scale; its rate constant was estimated to be about 2×10^7 s^{-1}. Brocklehurst and Young have demonstrated that the interconversion between excited ion pairs is not a universal process, the rate depending on the solvent and cation.[12]

To avoid the interference originating from ground state ion pairing we exploit the ultrafast proton transfer within the excited hydrogen bonded complex to selectively produce the excited contact ion pairs. Light absorption of the complex between N-methyl-3-hydroxynaphthalimide (3HONI) and 1-methyl-imidazole (MIm) (Scheme 1) results in strong dual

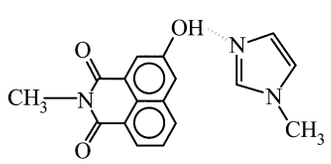

Scheme 1

fluorescence in media of moderate polarity and the two bands have been assigned to hydrogen bonded and solvent separated ion pairs.[13,14] The unique fluorescent behaviour and the fairly well separated emission bands in this system facilitate the investigation of the formation and decay processes of excited ion pairs in a wide temperature and solvent polarity range. We have recently revealed the viscosity effect on the kinetics of the reactions following the excited state proton transfer in 3HONI–MIm hydrogen bonded complex.[14] As an extension of these studies, the present paper focuses on the temperature effect in solvents of various polarity to clarify how the interaction with the medium influences the fluorescence, the radiationless energy dissipation and the reversible transitions of excited ion pairs.

† Dedicated to Professor Jean Kossanyi on the occasion of his 70th birthday.

 DOI: 10.1039/b209507f

Experimental

N-Methyl-3-hydroxy-1,8-naphthalimide (3HONI) was synthesised as described previously.[13] *N*-Methylimidazole and solvents (Aldrich, highest grade) were used without further purification. The UV-visible absorption spectra were obtained with a Varian-Cary model 50 Bio apparatus. Fluorescence spectra were recorded with SLM-Aminco model 8100 device. The temperature of the samples was controlled with an Oxford cryostat or a Lauda thermostatic bath. Fluorescence quantum yields were determined by comparison with that of 3-hydroxy-*N*-methyl-1,8-naphthalimide in CH_2Cl_2 solution, for which a reference yield of $\Phi_F = 0.13$ was taken.[13] Singlet lifetimes were measured by excitation with a B. M. Industries frequency-tripled Nd-YAG laser (pulse duration 30 ps FWHM), using the experimental set-up already described.[15]

Results and discussion

I Hydrogen bonding between 3HONI and MIm

As a representative example, Fig. 1 presents the change of the

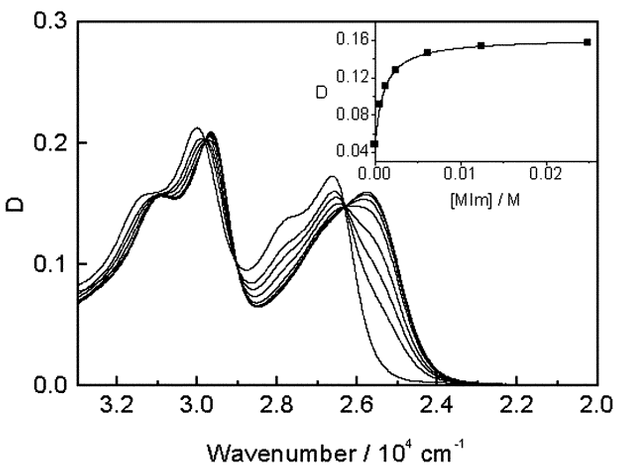

Fig. 1 Determination of the hydrogen bonding equilibrium constant in BuCl. Insert: change of the absorbance at 25770 cm^{-1}; the line presents the fitted function. [MIm] = 0, 6.21×10^{-4}, 1.242×10^{-3}, 2.484×10^{-3}, 6.21×10^{-3}, 1.242×10^{-2}, 2.484×10^{-2}, 6.21×10^{-2}M

absorption spectrum of 3HONI on addition of MIm in butyl chloride (BuCl). The gradual increase of the MIm concentration leads to bathochromic shift with clear isosbestic points at 29830, 29040 and 26320 cm^{-1}. The insert demonstrates that the change of the absorbance at a particular energy (A) can be well described assuming 1 : 1 hydrogen-bonded complex formation. Since the total concentration $[3HONI]_0$ is much smaller than $[MIm]_0$, the data are analysed using the following expression:

$$A = A_0(1 + K[\mathrm{MIm}]_0\, \varepsilon_C/\varepsilon_F)/(1 + K[\mathrm{MIm}]_0) \qquad (1)$$

where A_0 is the absorbance in the absence of MIm, $\varepsilon_C/\varepsilon_F$ denotes the ratio of the molar absorption coefficients for the complexed and free 3HONI. The non-linear least-squares fit of this function to the experimental data gives $K = 930$, 350 and 30 M^{-1} for the hydrogen bonding equilibrium constant in the ground state in BuCl, CH_2Cl_2 and butyronitrile (BuCN), respectively. The diminution of K in this series is partly due to the weakening of the hydrogen bond in more polar solvent and on the other hand, competitive hydrogen bonding with the solvent can also play significant role in butyronitrile.

II Fluorescence spectra and decays

The substantial red-shift of the absorption spectrum upon hydrogen bonding and the high equilibrium constant of MIm binding facilitate the selective excitation of 3HONI–MIm complex at 24690 cm^{-1}, where the free 3HONI has negligible absorption. Fluorescence spectroscopic studies were carried out with 3HONI solutions containing 0.062 M MIm in BuCl and CH_2Cl_2, whereas 0.155 M MIm was added in BuCN. Fig. 2

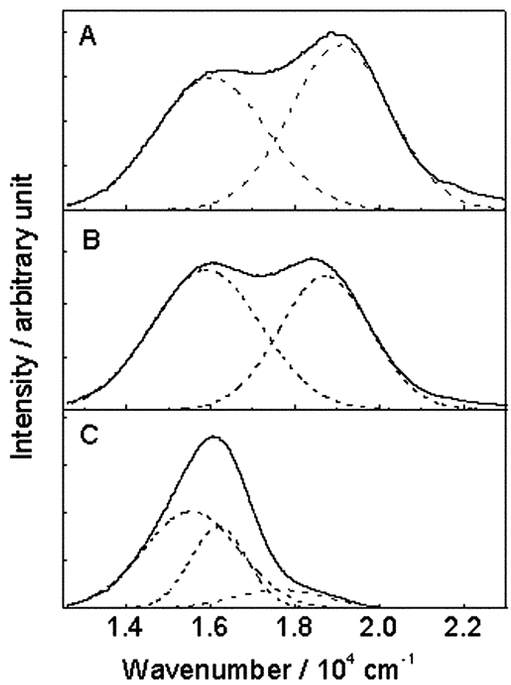

Fig. 2 Fluorescence spectra obtained by excitation of the 3HONI–MIm hydrogen bonded complex at 24690 cm^{-1} in BuCl at 290 K (A), CH_2Cl_2 at 294 K (B) and BuCN at 293 K (C). The bands are resolved by assuming Gaussian shape for the spectral components.

exhibits the fluorescence spectra recorded on excitation of the 3HONI–MIm hydrogen bonded complex. In BuCl and CH_2Cl_2 the spectrum comprises two superimposed bands which can be resolved by assuming Gaussian shape for the components. Light absorption of the 3HONI–MIm complex leads to ultrafast proton transfer along the hydrogen bond from the HO-moiety of naphthalimide to the imidazole ring (Scheme 2). The

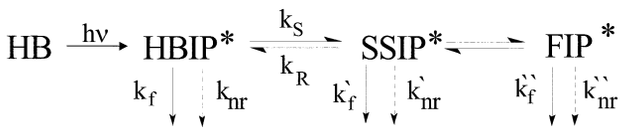

Scheme 2

emission band at higher energy is assigned to the excited hydrogen bonded ion pair (HBIP) formed in this process. The other band at lower energy is attributed to solvent separated ion pair (SSIP) in which each ion is fully solvated and Coulomb interaction prevents the separation. The spectrum is more complex in BuCN, where a third component seems to appear. The low energy band is composed of SSIP and free ion pair (FIP) emission. In this polar media the dissociation of SSIP is favoured because the high solvation energy expedites the further increase of the interionic distance. The SSIP ⟶ FIP transition is fairly fast, Gould and Farid reported 8×10^8 s^{-1} rate constant in acetonitrile.[16]

Fig. 2 demonstrates that the SSIP fluorescence becomes more intense compared to HBIP emission in more polar solvent and a concomitant bathochromic shift of the HBIP fluorescence maximum takes place. These facts indicate that the interaction with polar solvent decreases the energy of HBIP and promotes the conversion to SSIP. Cooling of the solution results in considerable change in the fluorescence spectra (Fig. 3). Although

Table 1 Temperature dependence of the fluorescence characteristics of 3HONI–MIm complex in BuCl: Maxima ($\bar{\nu}_{max}$), half-widths (HW), fluorescence yield ratios [Φ(SSIP)/Φ(HBIP)] and fluorescence decay parameters (λ_1, λ_2)

	HBIP		SSIP				
T/K	$\bar{\nu}_{max}$/cm^{-1}	HW/cm^{-1}	$\bar{\nu}_{max}$/cm^{-1}	HW/cm^{-1}	λ_1/10^8 s^{-1}	λ_2/10^8 s^{-1}	Φ(SSIP)/Φ(HBIP)
290	19080	1680	16020	1860	11.9	3.28	2.19
280	19070	1620	16080	1870	10.8	2.98	2.49
269	19070	1550	16150	1890	8.47	2.32	2.87
260	19070	1500	16200	1900	7.04	2.07	3.23
250	19060	1440	16240	1910	5.95	1.70	3.59
240	19050	1390	16280	1900	5.03	1.53	3.93
230	19040	1330	16330	1900	4.46	1.18	4.13
220	19030	1290	16360	1880	3.17	1.09	4.05
210	19010	1250	16400	1870	2.46	0.837	3.88
200	18990	1220	16470	1880	1.98	0.781	3.6
190	18960	1180	16600	1900	1.36	0.652	3.29
180	18920	1150	16760	1890	1.07	0.615	2.68
170	18870	1120	16930	1890	0.830	0.474	2.38
161	18820	1090	17170	1890	0.758	0.413	2.16

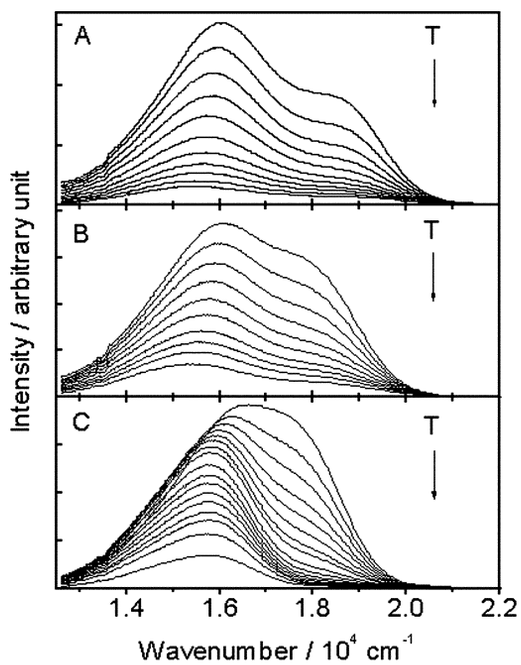

Fig. 3 Temperature dependence of the fluorescence spectra in BuCl (A), CH_2Cl_2 (B) and BuCN (C). The arrows show the direction of the temperature increase. The temperature ranges are 290–161 K (A), 294–180 K (B) and 293–165 K (C), respectively.

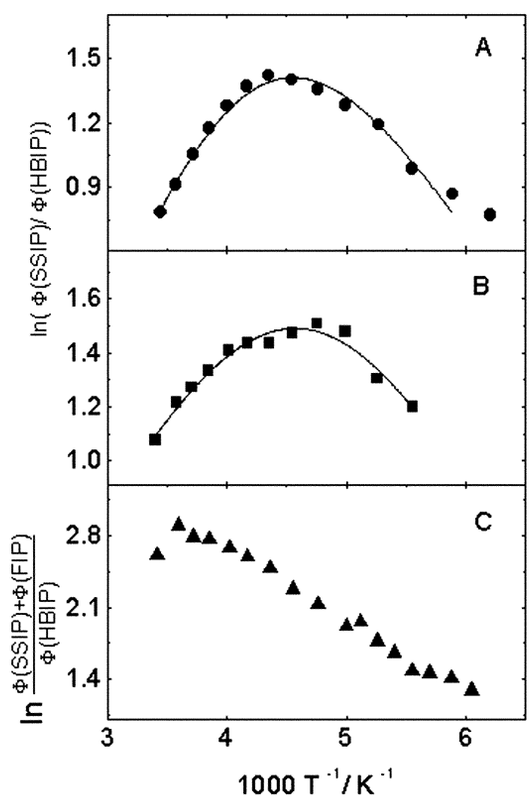

Fig. 4 Logarithm of the fluorescence yield ratios *vs.* the reciprocal temperature in BuCl (A), CH_2Cl_2 (B) and BuCN (C). Lines give the fitted function.

fluorescence enhancement is seen in the whole spectral range, the intensity ratio of the bands varies systematically with temperature. The spectra recorded in BuCl and CH_2Cl_2 can always be fitted with two Gaussian curves. It is seen in Table 1 and Table 2 that the half-width (HW) and the location of HBIP fluorescence maximum ($\bar{\nu}_{max}$), scarcely depend on temperature; however, going from 290 K to 180 K *ca.*1000 cm^{-1} blue shift is observed for the SSIP peak due to the deceleration of the solvent relaxation. The fluorescence yield ratio of the SSIP and HBIP species goes through a maximum upon lowering the temperature (Fig. 4A and 4B). This trend implies that the transition between the two excited species is a reversible process at high temperature where it is thermodynamically controlled (Scheme 2). Fluorescence intensity decays [$I(t)$] of HBIP and SSIP (monitored at 550 nm and 650 nm, respectively) can be well described with a sum of two exponentials:

$$I(t) = C_1 \exp(-\lambda_1 t) + C_2 \exp(-\lambda_2 t) \qquad (2)$$

where λ_1 and λ_2 are the decay parameters and C_1, C_2 denote the amplitudes. The short-lived decay component at 550 nm corresponded to the rise of the fluorescence recorded at 650 nm, whereas the long-lived components agreed at both wavelengths. The temperature dependence of the fitted λ_1, λ_2 values are given in Table 1 and Table 2.

In BuCN completely different fluorescent behaviour is found in the entire temperature range. The fluorescence decays cannot be fitted with dual exponential function and three Gaussian components are needed to resolve the spectra. These observations suggest that not only HBIP and SSIP but also FIP are present simultaneously even at low temperature. The intense fluorescence in the 18000–12500 cm^{-1} range is composed of the FIP and SSIP emission. Fig. 4C exhibits the logarithm of the fluorescence yield ratio [Φ(FIP) + Φ(SSIP)]/Φ(HBIP) in the function of the reciprocal temperature in BuCN. Analogous plots of the ln[Φ(SSIP)/Φ(HBIP)] data measured in BuCl and CH_2Cl_2 show completely different reciprocal temperature dependence (Fig. 4A and 4B). The large number of reaction

Table 2 Temperature dependence of the fluorescence characteristics of 3HONI–MIm complex in CH_2Cl_2: Maxima ($\bar{\nu}_{max}$), half-widths (HW), fluorescence yield ratios [Φ(SSIP)/Φ(HBIP)] and fluorescence decay parameters (λ_1, λ_2)

	HBIP		SSIP				
T/K	$\bar{\nu}_{max}$/cm^{-1}	HW/cm^{-1}	$\bar{\nu}_{max}$/cm^{-1}	HW/cm^{-1}	λ_1/10^8 s^{-1}	λ_2/10^8 s^{-1}	Φ(SSIP)/Φ(HBIP)
294	18720	1530	15900	1830	7.50	1.86	2.94
280	18710	1440	16030	1880	5.81	1.51	3.37
270	18700	1390	16110	1910	4.77	1.40	3.57
260	18690	1350	16180	1930	3.92	1.25	3.80
249	18670	1300	16260	1950	3.22	1.09	4.09
240	18650	1260	16340	1970	2.67	0.988	4.20
230	18620	1230	16420	1980	2.17	0.913	4.21
220	18590	1190	16530	2020	1.90	0.863	4.36
210	18560	1500	16670	2060	1.42	0.774	4.52
200	18500	1130	16780	2090	1.07	0.722	4.48
190	18440	1100	16950	2060	0.86	0.634	3.69
180	18370	1080	17040	2040	0.66	0.521	3.32

Table 3 Kinetic and thermodynamic parameters

Solvent	Dielectric constant	k_f/ 10^7 s^{-1}	k_{nr}/ 10^7 s^{-1}	A_S/ 10^{12} s^{-1}	E_S/ kJ mol^{-1}	A_R/ 10^{12} s^{-1}	E_R/ kJ mol^{-1}	k'_f/ 10^7 s^{-1}	A'_{nr}/ 10^{10} s^{-1}	E'_{nr}/ kJ mol^{-1}	$-\Delta S$/ JK^{-1} mol^{-1}	$-\Delta H$/ kJ mol^{-1}
Ethyl acetate[a]	6.0[b]	1.1	1.1	4.7	15.8	1090	30.6	2.4	0.47	7.2	45	15
BuCl	7.2[c]	0.64	3.1	0.13	11.2	12	22.4	1.5	0.25	6.1	38	11
CH_2Cl_2	8.9[b]	0.32	1.7	0.042	10.2	0.95	17.1	1.5	0.088	4.6	26	7

[a] Calculated from the data in ref. 14. [b] Ref. 18. [c] Ref. 19.

steps with different temperature dependence prevents the kinetic analysis of the data presented in Fig. 4C.

III Evaluation of temperature dependent results

Kinetic parameters of the reactions can be determined from the results of the steady-state and time-resolved fluorescence studies in BuCl and CH_2Cl_2 where no indication appears for FIP formation and therefore, the reaction scheme is more simple. The fluorescence yield ratio Φ(SSIP)/Φ(HBIP) diminishes below 230 and 210 K in BuCl and CH_2Cl_2, respectively (Table 1 and Table 2) because the rate constant of the endothermic transition from SSIP to HBIP (k_R) becomes much lower than the reverse reaction and SSIP formation significantly slows down. Hence, in this low temperature domain the fluorescence decay parameters are defined as follows:

$$\lambda_1 = k_f + k_{nr} + k_S \quad (3)$$

$$\lambda_2 = k'_f + k'_{nr} \quad (4)$$

where k_S, k_f and k_{nr} represent the rate constant of SSIP formation, fluorescence and non-radiative deactivation for HBIP, respectively; the primed quantities refer to the corresponding processes for SSIP. Eqn. (3) is valid if $k_S >> k_R$, whereas eqn. (4) is a good approximation if $k'_f + k'_{nr}$ is much larger than k_R. Taking the kinetic parameters summarised in Table 3, we calculated k_S/k_R and $(k'_f + k'_{nr})/k_R$ ratios at 200 K. The former ratio was 31, 9 and 3, while the latter ratio gave 7.7, 4.6 and 2.2 in ethyl acetate (EtOAc), BuCl and CH_2Cl_2, respectively. These values confirm that eqns. (3) and (4) are fair approximations below 200 K. Global fit of the time-resolved and the steady-state fluorescence data below 200 K helped to increase the precision of the derived parameters in CH_2Cl_2, where k_R is not completely negligible.

Table 1 and Table 2 show that neither λ_1 nor λ_2 is constant at low temperature. The following expressions give the temperature dependence of the decay parameters:

$$\lambda_1 = k_f + k_{nr} + A_S \exp(-E_S/RT) \quad (5)$$

$$\lambda_2 = k'_f + A'_{nr} \exp(-E'_{nr}/RT) \quad (6)$$

where A_S, E_S and A'_{nr}, E'_{nr} are the Arrhenius parameters for the formation and the radiationless deactivation of SSIP, respectively. The results of the non-linear least-squares fits are compiled in Table 3.

The fact that λ = constant + $A \exp(-E/RT)$ type function well describes the change of measured λ_1 and λ_2 values in the low temperature range indicates the temperature independent character of the radiative rate constants (k_f, k'_f) and the radiationless relaxation of excited HBIP to the ground state (k_{nr}). Therefore, based on Scheme 2, the following relationship can be derived to describe the experimental results given in Fig. 4A and 4B:

$$\ln\frac{\Phi(\mathrm{SSIP})}{\Phi(\mathrm{HBIP})} = \ln\frac{k'_f A_S \exp(-E_S/RT)}{k_f[k'_f + A_R \exp(-E_R/RT) + A'_{nr} \exp(-E'_{nr}/RT)]} \quad (7)$$

Using the kinetic parameters determined from the fluorescence decays at low temperature, there are only three unknown quantities in this relation: the rate constant of HBIP fluorescence (k_f), and the Arrhenius factors (A_R, E_R) of the back formation of HBIP. These kinetic parameters can be determined by non-linear least-squares fit of eqn. (7) to the temperature dependence of ln[Φ(SSIP)/Φ(HBIP)]. The parameter values corresponding to the best fit are summarised in Table 3 and the lines in Fig. 4A and 4B represent the calculated functions. The enthalpy (ΔH) and entropy change (ΔS) in the reversible transition between HBIP and SSIP is obtained from the expressions:

$$\Delta H = E_S - E_R \quad (8)$$

$$\Delta S = R(\ln A_S - \ln A_R) \quad (9)$$

IV Solvent effect on kinetic and thermodynamic parameters

Based on the data in Table 3, we can infer which reaction steps exhibit solvent dependence. The dielectric constant (ε) is

utilised to characterise the polarity of the media. Going from EtOAc ($\varepsilon = 6.0$) to CH_2Cl_2 ($\varepsilon = 8.9$) the most substantial change appears in the Arrhenius parameters of the SSIP ⟶ HBIP process where the A-factor diminishes more than three orders of magnitude and the activation energy lessens by 13.5 kJ mol^{-1}. Somewhat less effect is found for the HBIP ⟶ SSIP reaction: about two orders of magnitude decrease is seen in A_S, whereas E_S is *ca.* 55% lower in CH_2Cl_2 than in EtOAc. The considerable diminution of the A-factors implies that the structure of the transition state is very sensitive to the solvent polarity. In EtOAc, where the solvent molecules are weakly oriented, the enlarged distance within the ion pair in the transition state results in positive activation entropy for the HBIP ⟶ SSIP process and the transition state resembles more the HBIP. In contrast, in solvents of higher dipole moment the entropy increase due to the detachment of the ions is compensated with the entropy decrease arising from the more oriented solvent shell in the transition state. Because of the better solvation, the structure of the transition state becomes gradually more similar to the SSIP as the polarity of the medium grows.

Also the thermodynamic parameters of the reversible conversion between HBIP and SSIP clearly show correlation with the dielectric constant of the solvent. The solvent molecules are less ordered and weaker bound around HBIP compared to SSIP because the shorter interior distance in the former case leads to cancellation of the orienting influence of the ions. However, in a polar solvent, even the HBIP becomes better solvated and the difference in the extent of orientation for the solvate shell of HBIP and SSIP diminishes. Therefore, the entropy change in the HBIP ⟶ SSIP reaction is less negative in a polar solvent. The SSIP formation proved to be an exothermic process in all solvents (Table 3) because the release of energy arising from the better solvation of the SSIP outweighs the electrostatic work that is needed for the separation of the HBIP.

The radiative rate constants are represented by

$$k_F = \frac{64\pi^4 n^3}{3h} \bar{\nu}_F{}^3 M^2 \qquad (10)$$

where $\bar{\nu}_f^3$, h, n and M are the average fluorescence wavenumber, the Planck constant, the refractive index of the medium and the transition moment for fluorescence, respectively. Since the fluorescence maxima barely shift in various solvents, the more substantial solvent dependence of k_F compared with k_F' is a consequence of the larger solvent effect on the transition moment of HBIP fluorescence. Considerable solvent polarity effect was reported also for the radiative rate constant of the singlet excited intramolecular electron donor–acceptor systems.[17]

From the internal conversion processes only the one depopulating the excited SSIP has temperature dependent rate. The activation energy of this transition is scarcely influenced by the solvent, however, about 5-fold decrease is observed for the A-factor with increasing dielectric constant of the medium. Temperature dependent non-radiative decay has been found also for excited fluorenyl salts[12] and the Arrhenius parameters reported in that case agree with the results shown in Table 3.

The observation that the radiationless relaxation of excited HBIP to the ground state is temperature independent while the same process from SSIP is energy activated, can be rationalised based on the energy gap law. Table 1 and Table 2 as well as ref. 14 demonstrate that the fluorescence maximum of HBIP barely shifts at various temperatures but that of SSIP moves towards a higher wavenumber upon cooling. As the excited state energy of the former species does not change, temperature independent internal conversion is expected based on the energy gap law in agreement with the experimental results. However, in the case of SSIP cooling of the solution enhances the excited state energy and the diminution of the vibrational coupling caused thereby can lead to temperature dependent internal conversion. The blue shift of the SSIP fluorescence band with diminishing temperature probably indicates that ΔH is temperature dependent. Hence, the calculated thermodynamic and Arrhenius parameters could be regarded as the averages of the corresponding values in the entire temperature range.

It is worth pointing out that the solvent polarity effect on the fluorescence maximum of SSIP is extraordinarily small (Table 1 and Table 2). The red shift of the SSIP peak relative to the HBIP peak is also scarcely sensitive to the solvent: 3210, 3060, 2820 cm^{-1} were obtained at room temperature in EtOAc, BuCl and CH_2Cl_2, respectively. This slight decrease with increasing solvent polarity agrees with the trend shown for ΔH in Table 3. Our results suggest that entropy effects play dominant role in the formation and stabilisation of the excited SSIP.

Acknowledgements

L. B. very much appreciates the support of this work by the 1/047 NKFP Medichem Project and the Hungarian Scientific Research Fund (OTKA, Grant T034990).

References

1 (*a*) M. Szwarc, *Carbanions Living Polymers and Electron Transfer Processes*, Wiley-Interscience, New York, 1968; (*b*) *Ions and Ion Pairs in Organic reactions*, ed. M. Szwarc, Wiley-Interscience, New York, 1972; (*c*) T. E. Hogen-Esch, *Adv. Phys. Org. Chem.*, ed. V. Gold, Academic Press, London, 1977, vol. 15, pp. 153–266.
2 S. Winstein, E. Clippinger, A. H. Fainberg and G. Robinson, Salt effects and ion-pairs in solvolysis, *J. Am. Chem. Soc.*, 1954, **76**, 2597–2598.
3 H. Sadek and R. Fuoss, Electrolyte–solvent interaction. IV. Tetrabutylammonium bromide in methanol–carbon tetrachloride and methanol–heptane mixtures, *J. Am. Chem. Soc.*, 1954, **76**, 5897–5909.
4 Y. Marcus, *Ion solvation*, Wiley, New York, 1985.
5 P. Vandereecken, J.Ph. Soumillion, M. Van Der Auweraer and F. C. De Schryver, The photophysics of alkali naphtholates: lifetimes of contact and solvent-separated ion pairs present simultaneously in weakly polar solvents, *Chem. Phys. Lett.*, 1987, **136**, 441–446.
6 J. Ph. Soumillion, P. Vandereecken, M. Van Der Auweraer, F. C. De Schryver and A. Schanck, Photophysical analysis of ion paring of β-naphtholate in medium polarity solvents: Mixtures of contact and solvent-separeted ion pairs, *J. Am. Chem. Soc.*, 1989, **111**, 2217–2225.
7 A. K. Mishra and H. Shizuka, Dual emission from the contact and separated ion pairs in polyethylene films at 77 K, *Chem. Phys. Lett.*, 1988, **151**, 379–383.
8 A. K. Mishra, M. Sato, H. Hiratsuka and H. Shizuka, Dual emission from ion pairs produced by excited-state proton transfer in the naphthol–amine system at 77 K, *J. Chem. Soc., Faraday Trans.*, 1991, **87**, 1311–1319.
9 A. K. Mishra and H. Shizuka, Temperature effects on dual emission from ion pairs produced by excited proton transfer in the 1-naphthol-triethylamine system, *J. Chem. Soc., Faraday Trans.*, 1996, **92**, 1481–1486.
10 H. W. Vos, H. H. Blom, N. H. Velthorst and C. MacLean, A spectroscopic study of carbanions and corresponding nitranions: Ion pair formation in the ground state and the first excited state, *J. Chem. Soc., Perkin Trans. 2*, 1972, 635–639.
11 T. E. Hogen-Esch and J. Plodinec, Ion pairing in excited states of carbanions. 2. Emission of fluorenyl alkali salts in aprotic media, *J. Am. Chem. Soc.*, 1978, **100**, 7633–7640.
12 B. Brocklehurst and R. N. Young, The fluorescence of ion pairs of the fluorenyl carbanion, *Phys. Chem. Chem. Phys.*, 2001, **3**, 3018–3026.
13 L. Biczók, P. Valat and V. Wintgens, Effect of molecular structure and hydrogen bonding on the fluorescence of hydroxy-substituted naphthalimides, *Phys. Chem. Chem. Phys.*, 1999, **1**, 4759–4766.
14 L. Biczók, P. Valat and V. Wintgens, Ion pair formation *via* photoinduced proton transfer in excited hydroxynaphthalimide-*N*-methylimidazole hydrogen bonded complex: Effect of temperature and viscosity on dual fluorescence, *Phys. Chem. Chem. Phys.*, 2001, **3**, 1459–1464.

15 P. Valat, V. Wintgens, J. Kossanyi, L. Biczók, A. Demeter and T. Bérces, Influence of geometry on the emitting properties of 2,3-naphthalimides, *J. Am. Chem. Soc.*, 1992, **114**, 946–953.
16 I. R. Gould and S. Farid, Fluorescence of excited charge-transfer complexes and absolute dynamics of radical-ion pairs in acetonitrile, *J. Phys. Chem. A.*, 1992, **96**, 7635–7640.
17 E. M. Kosower, H. Dodiuk and H. Kanety, Intramolecular donor–acceptor systems. 4. Solvent effects on radiative and non-radiative processes for the charge transfer states of *N*-arylamino-naphthalene-sulfonates, *J. Am. Chem. Soc.*, 1978, **100**, 4179–4188.
18 C. Reichardt, *Solvent effects in organic chemistry*, Verlag Chemie, Weinheim, New York, 1979, p. 271.
19 M. Maus, W. Rettig, D. Bonafoux and R. Lapouyade, Photoinduced intramolecular charge transfer in a series of differently twisted donor–acceptor biphenyls as revealed by fluorescence, *J. Phys. Chem. A.*, 1999, **103**, 3388–3401.